Proceedings of SPIE: Laser interferometry IX: Techniques and Analysis,
20-21 July 1998, San Diego, CA, USA.
DOI:10.1117/12.312976

Three-dimensional Shape Measurement using Fibre Optic Low Coherence Speckle Interferometry

Itziar Balboa and Ralph P. Tatam

Optical Sensors Group, Centre for Photonics and Optical Engineering, School of Mechanical Engineering, Cranfield University, Cranfield, Bedford, MK43 0AL, U.K.

1. ABSTRACT

A low coherence speckle interferometer implemented using single mode optical fibre and a multimode laser diode as a pseudo-low coherence source is described. The design of the interferometer is presented and demonstrated on simple test objects. Signal processing techniques to improve the performance of the system are discussed.

Keywords: speckle interferometry, low coherence sources, surface profile measurement.

2. INTRODUCTION

Speckle Interferometry is a generic term for a range of optical configurations that utilise speckles, generated by the interference of light scattered from different points on an optically rough surface, to convey information about the object surface[1-3]. Information on the in-and out-of-plane surface strain components, vibrational characteristics and surface profile is available simultaneously over an extended area of the object surface. Shape information is a requirement in many engineering applications. For example, on-line quality control, solid modelling (the transfer of contour information from prototypes to CNC machines), biomedical applications, and the measurement of surface wear. In addition, for objects with non-planar shapes, surface contour and slopes are required for a complete strain analysis[4, 5].

Various full-field optical methods have been developed for contour and slope measurement, for example, moiré holographic interferometry, fringe projection, electronic speckle pattern interferometry (ESPI) and shearography. The techniques employed for speckle methods were originally developed from those of holographic interferometry and include refractive index change of the medium surrounding the object, tilting the object[6,7], two-wavelength illumination[8,9] and two source illumination[10,11] produced by shifting or tilting the illumination. All these techniques produce fringes that represent height contours on the object surface. In speckle interferometry the two wavelength and the two source techniques are most applicable to engineering applications.

All these techniques use laser sources with relatively long coherence lengths (10^{-2}-10^{2}m). More recently, there has been a growing interest in using low coherence techniques[12,13] in speckle interferometry[14,15]. In low coherence speckle interferometry (LCSI) sources with short coherence lengths, usually <100μm are employed. Interferometric speckles are only observed when the optical path length (OPL) in the reference arm of the interferometer matches the OPL in the signal arm, i.e. the one containing the test surface. By changing the OPL in the reference arm, interferometric speckles are obtained at different locations on the test object. The resolution of the technique can be a few micrometers with a range of several hundred millimetres, implying a dynamic range of $\sim 10^{5}$. Reported arrangements have utilised conventional optical components with continuous wave illumination[14] and with short pulsed illumination[15].

In this paper we describe a low coherence speckle interferometer (LCSI) using single mode optical fibre technology and demonstrate its potential for shape measurement of large object areas. The use of single mode optical fibre increases the robustness and versatility of the technique as well as providing inherent spatial filtering of the beams.

Low coherence sources that have been used include gas discharge lamps and light emitting diodes (LEDs). However the very low brightness of these sources produces inefficient coupling into single mode optical fibre. In a previous paper[16] we investigated solid state sources suitable for LCSI applications and demonstrated that multimode laser diodes (MMLDs) can

Part of the SPIE Conference on Laser Interferometry IX: Techniques and Analysis • San Diego, California • July 1998
SPIE Vol. 3478 • 0277-786X/98/$10.00

be used as quasi-white light sources with the major advantage compared to superluminescent diodes (SLDs) of higher power operation, typically several tens of mW.

3. THEORY

In low coherence interferometry, often termed, "white light" interferometry, the fringe visibility is a function of the optical path difference and can be obtained as the Fourier transform of the spectral intensity distribution[17]. The following expression describes the usual cosine function from a two beam interferometer but with an additional Gaussian envelope function modulating the fringe intensity[18]. The form of the transfer function shown in figure 2, is given by

$$I_N(x)=\left(\frac{1}{2}\right)\left\{1+\exp\left(-\left(\frac{2x}{L_C}\right)^2\right)\cos\left(\frac{2\pi x}{\bar{\lambda}}\right)\right\} \tag{1}$$

where I_N represents the normalised signal intensity, L_C is the coherence length of the source, $\bar{\lambda}$ is the central wavelength of the source and x is the relative optical path difference of the interferometer. Equation 1 states that the shorter the source coherence length the more rapidly the cosine fringe intensity is reduced.

For speckle systems, the fringes are the result of the correlation of two speckle patterns. When a low coherence source is employed, interferometric speckles are only obtained if the optical path length difference between the two arms of the interferometer, i.e. (test and reference arms) is within the coherence length of the source. For the case of the MMLD, the interference pattern is the result of the contribution of each individual mode of the spectrum of the laser modulated by another "envelope function". This function will be Gaussian if the source spectral profile is Gaussian.

Considering the spectral envelope of a multimode laser diode as a Gaussian distribution and the spectral shape of a single lasing mode as Lorentzian[19] (see fig. 3), the total intensity due to the contribution of all the modes can be expressed as follows:

$$\begin{aligned} I &= \sum_{j=-m}^{m} I_j = \sum_{j=-m}^{+m} \exp\left[-2\pi\left(j\frac{\Delta\sigma}{\delta\sigma}\right)^2 - \delta'\sigma x/2\right]\cos\left(2\pi x\sigma_j + \phi_s\right) \\ &= \exp\left(\delta'\frac{\sigma x}{2}\right)\sum_{j=-m}^{m}\exp\left[-2\pi\left(j\frac{\Delta\sigma}{\delta\sigma}\right)\right]\cos\left(2\pi x\sigma_j + \phi_s\right) \end{aligned} \tag{2}$$

where m is the order of the lasing modes, $\Delta\sigma$ is the difference between adjacent mode wave numbers, $\delta\sigma$ is the full width at half maximum height of the envelope, σ is the wave number of the source, σ_j is the wave number of the jth lasing mode, $\delta'\sigma$ is the spectral width of the lasing mode, x is the optical path difference in the interferometer, and ϕ_s is the randomly varying speckle phase. Figure 4 shows a plot of the zero order and two adjacent orders that would be obtained by scanning a Michelson interferometer illuminated by a MMLD. The brightest (zero order) fringes are obtained at zero path length imbalance. Lower intensity fringes are formed at non-zero path length imbalance. The separation of the fringe "packets" is equal to the optical path length of the laser cavity. Typically for solid state laser diodes this is approximately 1mm. Due to the poor spatial resolution of the CCD camera it is not possible to see the fringes inside each of the intereference envelopes. Instead, the low coherence interferometric speckle fringes are represented by bands, each one of different intensity, where the zero order (zero path length imbalance) has the highest intensity.

4. EXPERIMENTAL ARRANGEMENT

The experimental configuration employed is shown in Fig.1. Light from a 40mW multimode laser diode (Sony SLD201U-3) operating at 792nm, is coupled into a variable split ratio single mode directional coupler, fabricated in our laboratories. The variable split ratio enables optimization of the distribution of light in the interferometer; more than 95% is used to illuminate the test object.

The light scattered from the test surface is collected by a zoom lens and imaged onto a CCD camera via a 90/10 beamsplitter. The optical path for the reference beam is as follows: the transmitted light from one of the ports of the coupler is directed to a mirror. A microscope objective is placed in front of the mirror to collimate the beam. The mirror is mounted on a translation stage with a travel of up to 75mm and step resolution of 10nm.

In speckle interferometry it is important to optimize the speckle size with respect to the pixel size of the CCD camera. The expression for the speckle diameter, S, is given by [20]:

$$S = 1.2(1+M)\lambda F \tag{3}$$

where λ is the wavelength of the source, M is the magnification of the lens in the imaging optics and F represents the f-number of the lens. For a wavelength of 792nm, a magnification of 0.25 and a pixel size of 126.5μm^2 an optimum aperture is F 11.

4.1 Image and Signal Processing

The interferograms are captured by the CCD and an image processing board housed in a PC. The speckle pattern can be displayed live on a TV monitor, which generally shows speckles across the entire object surface. Information on the object shape can only be obtained from the interferometric speckles, which can be distinguished from the non-interferometric speckles as they have a higher intensity.

In order to increase the speed of the data processing and improve the interferometric speckle contrast it is convenient to eliminate the non-interferometric speckles. This is achieved using real time digital image subtraction[21,22]. This method involves the subtraction of images of two consecutive speckle patterns with a π phase shift added between them. Consequently, only interferometric speckles can be observed and the rest of the image appears black.

A piezo electric transducer (PZT) attached to the mirror is used to provide the π phase shift. The DC motor translation stage is used to scan the OPL of the reference arm of the interferometer. By continuously translating the mirror, it is possible to observe the interferometric speckles move across the object surface. As the mirror is translated, the intensity value for each pixel is compared with its previous value. The highest value is stored along with the corresponding position of the translation stage. In this way a 3D map of the object surface is built up.

4.2 Calibration of the optical path length imbalance

The optical path difference between the reference and the test beams was calibrated using a source-wavelength modulation technique[23]. The purpose of this calibration is to keep the optical path length imbalance of the interferometer to less than 40mm as this is the range of the translation stage.

The experimental arrangement is the same as in fig. 1, however the source is now a single mode laser diode (SDL 5411-G1) operating at 806nm and 100mW optical power output. A Faraday isolator was used to prevent feedback into the laser cavity.

Modulation of the injection current produces a concomitant change in the laser diode emission wavelength[24,25]. In an interferometer with a path length imbalance x this produces a phase change, $\Delta\phi$, given by:

$$\Delta\phi = \frac{2\pi}{c} x \Delta\nu \qquad (4)$$

where $\Delta\nu$ is the change in the optical frequency and c is the free space speed of light. The optical frequency modulation of the laser was measured using a confocal Fabry-Pérot interferometer to be 1.4 ± 0.1GHz/mA. This value is then used in the previous equation to calculate the optical path length (OPL) imbalance, in the following manner. A speckle image of the test object is acquired and stored. The object is then deformed and subsequent images subtracted from the reference image and the results displayed. The object was deformed to produce approximately 10 tilted fringes across the field of view. Changing the laser wavelength causes the fringes to move. To facilitate the measurement the laser diode injection current was modulated at 0.5Hz and the amplitude varied until a 2π phase change had been achieved. The OPL imbalance measured was approximately 15mm for a $\Delta\nu$ of 21.4 GHz.

5. RESULTS AND DISCUSSION

Two different test objects were investigated. The first was a circular plate, sprayed matt white, of 50mm diameter tilted at angle of 11°± 1° relative to the axis of the receiving optics. The second object was a gas turbine compressor blade which measured approximately 170mm in height, 110mm in width and had an overall depth of approximately 40mm. The blade was covered with retroreflective tape.

As discussed in section 4.1, the measurement of individual pixel intensity is associated with a particular mirror position. The resolution of this technique is dictated by the separation of the mirror position between measurements, as this determines the uncertainty in the depth value for each pixel. In this experiment the measurement process was not completely automated. As this approach is time consuming fewer points were taken reducing the resolution of the system to approximately 0.2mm for the disc and 0.1mm for the blade. However for an automated measurement process the mirror steps can be reduced to a couple of microns and the whole process should take approximately 1 hour to map out an object with a depth of 100mm to a resolution of ~1μm.

Figure 5 shows the 3D representation of the disk. The 50mm diameter disk was orientated at an angle of 11° with respect to the center axis of the receiving lens implying an overall depth (z axis) of 9.5±0.9mm. The depth recovered from the LCSI was 9.7±0.2mm demonstrating good agreement between the two measurements.

The three figures (see fig. 6) represent low coherence speckle fringes at different positions on the surface of the blade. The value of x shows the distance in millimeters that the reference mirror has moved between each image. Several fringes can be observed in each image due to the discrete modal characteristics of the MMLD. The fringe spacing measured from the images was approximately 1mm in good agreement with the theoretical value of 1.05mm obtained for a 300μm cavity length and a group index of 3.5.

Figure 7 shows a 3D plot of the surface of the blade (see fig. 7). The x and y axes represent the illuminated area and the z axis the depth value. A slope change across the object surface can be distinguished consistent with the blade geometry.

As speckle is an inherently noisy process, improvement in the images can be obtained using phase shifting[26] and speckle averaging techniques[27]. This will be investigated further in conjunction with automation of the data collection.

6. CONCLUSIONS

A low coherence speckle interferometer employing a MMLD and single mode optical fibre has been demonstrated. The application of this technique has been examined to study relatively large surface areas. The resolution is in the range of 0.1mm. Techniques to improve the accuracy and the measurement speed have been discussed.

7. ACKNOWLEDGEMENTS

The authors are grateful to the Paul Instrument Fund of the Royal Society, U.K for supporting this work.

8. REFERENCES

1. R. Jones & C. Wykes, *Holographic and Speckle Interferometry*, Cambridge University Press, Cambridge, 2nd ed., 1989.
2. J. A. Leendertz, "Interferometric Displacement Measurement on scattering surfaces utilising Speckle Effect", *J. Physics. E:Sci. Instrum*, **3**, pp. 214-218, 1970.
3. O. J. Løckberg and P. Svenke, "Design and use of an Electronic Speckle Pattern Interferometer for testing of turbine parts", *Opt. and Lasers in Eng.*, **2**, pp. 1-12, 1981.
4. Y. Y. Hung, J. L. Turner, M. Tafralian, J. D. Hovanesian, C. E. Taylor, "Optical method for measuring contour slopes of an object", *Appl. Opt.*, **17**, 1, pp. 128-131, 1978.
5. S. Winther, "3D Strain measurements using ESPI", *Optics and Lasers in Engineering*, **8**, pp. 45-47, 1988.
6. G. K. Jaisingh & F. P. Chiang, "Contouring by laser speckle", *Appl. Opt.*, **20**, 19, pp.3385-3387, 1981.
7. A. R. Ganesan & R. S. Sirohi, "New method of contouring using digital speckle pattern interferometry (DSPI)", *SPIE*, **954**, pp. 327-332, 1988.
8. R. P. Tatam, J. C. Davies, C. H. Buckberry and J. D. C. Jones, "Holographic surface contouring using wavelength modulation of laser diodes", *Optics & Laser Technology*, **22**, 5, pp. 317-321, 1990.
9. A. F. Fercher, Z. Hugh and Vry, "Rough surface interferometry with a two-wavelength heterodyne speckle interferometer", *Appl. Opt.*, **24**, pp. 2181-2188, 1985.
10. X. Peng, H. Y. Diao, Y. L. Zou and Tiziani, "Contouring by modified dual-beam ESPI based on tilting illumination beams", *Optik*, **90**, 2, pp. 61-64, 1992.
11. B. D. Bergquist and P. Montgomery, "Contouring by electronic speckle pattern interferometry (ESPI)", *SPIE*, **473**, pp. 44-47, 1984.
12. H. C. Lefevre, "White Light Interferometry in Optical Fiber Sensors", Proceedings of Seventh Optical Fiber Sensors Conference Iree, Sydney, pp. 345-351, 1990.
13. Y. Rao and D. A. Jackson, "Recent progress in fibre optic Low- Coherence Interferometry", *Meas. Sci. Technol.* **7**, pp. 981-999, 1986.
14. T. Dresel, G. Haüsler and H. Venzke, "Three dimensional sensing of rough surfaces by coherence radar", *Appl. Opt.*, **31**, no. 7, pp. 919-925, 1992.
15. A. Wei and T. E. Carlsson, "Direct object-shape comparison by light-in-flight speckle interferometry", *Optics Letters*, **22**, 20, pp. 1538-1540, 1997.
16. I.Balboa and R. P. Tatam, "Source considerations for Low Coherence Speckle Interferometry", *Proc. SPIE,* **3098**, pp. 316-324, 1997.
17. M. Born and E. Wolf, *Principles of Optics*, 6th ed., New York: Pergamon, 1986.
18. D. N. Wang, Y. N. Ning, K. T. V. Grattan, A. W. Palmer and K. Weir, "The optimized wavelength combinations of two broad-band sources for White Light Interferometry", *Journal of Light wave Technology*, **12**, 5, pp. 909-915, 1994.
19. Y. Ning, K. T. V. Grattan, B. T. Meggitt, and A. W. Palmer, "Characteristics of laser diodes for interferometric use", *Appl. Optics.*, **28**, 17, pp. 3657-3661, 1989.
20. A. E. Ennos, Speckle Interferometry. Coherent Optical Engineering, ed. F. T. Arecchi and V. Degiorgio, North Holland Publishing Company, pp. 129-149, 1977.
21. S. E. Moran, R. L. Law, P. N. Craig, W. M. Goldberg, "Optically phase locked Electronic Speckle Pattern Interferometry", *Appl. Opt*, **26**, pp. 475-491, 1987.
22. J. C. Davies, and C. H. Buckberry, "Application of electronic speckle pattern interferometry in automotive product development", VDI Berichte, 617, pp. 279-293, 1986.
23. A. Olszak, R. P. Tatam, "The calibration of the optical-path length imbalance in optical fibre ESPI systems employing source-wavelength modulation", *Meas. Sci. Technol.*, **8**, pp. 759-763, 1997.
24. H. D. Ford, H. Atcha and R. P. Tatam, "Optical fibre technique for the measurement of small frequency separations: application to surface profile measurement using electronic speckle pattern interferometry", *Meas. Sci. Technol.*, **4**, pp. 601-607, 1993.

25. A. Dandridge and L. Goldberg, "Current induced frequency modulation in diode lasers", *Electron. Lett.*, **18**, pp. 302-304.
26. K. Creath, "Phase-shifting speckle interferometry", *Appl. Opt.*, **24**, 18, pp., 3053-3058.
27. E. Vikhagen, O. Løckberg, "Speckle averaging in deformation analysis using video speckle interferometry", *Optics and Lasers in Engineering*, **27**, pp. 179-190, 1987.

Further author information:
R. P. Tatam: Email: r.p.tatam@cranfield.ac.uk, telephone: +441234 754630, fax: +441234 750728

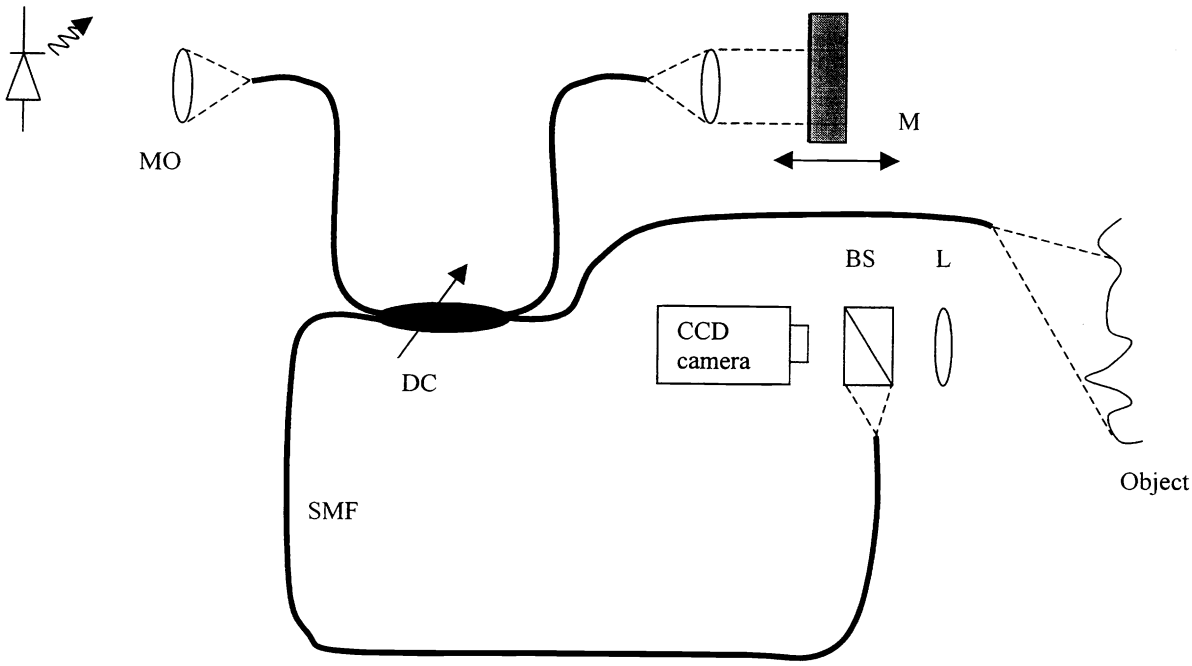

Fig. 1: Experimental arrangement for a fibre optic low coherence speckle interferometer. BS: beam-splitter, DC: variable split ratio directional coupler, L: zoom lens, M: mirror, MO: microscope objective, SMF: single mode optical fibre.

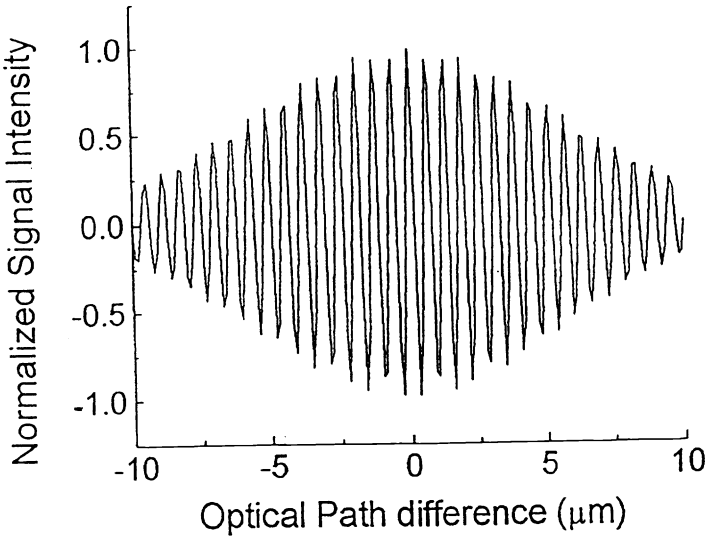

Fig. 2: White light interferogram

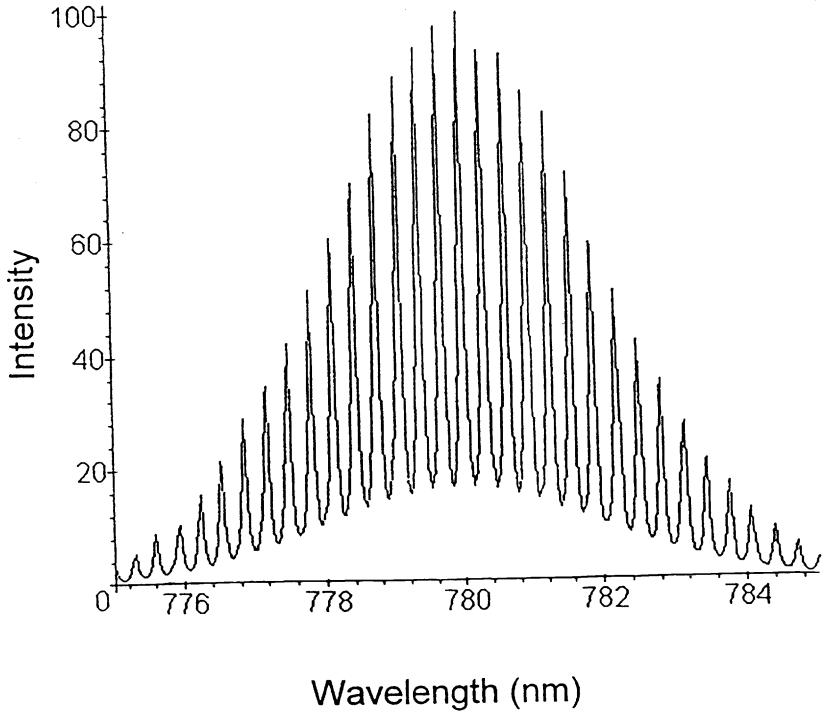

Fig. 3: Theoretical spectrum of a multimode laser diode.

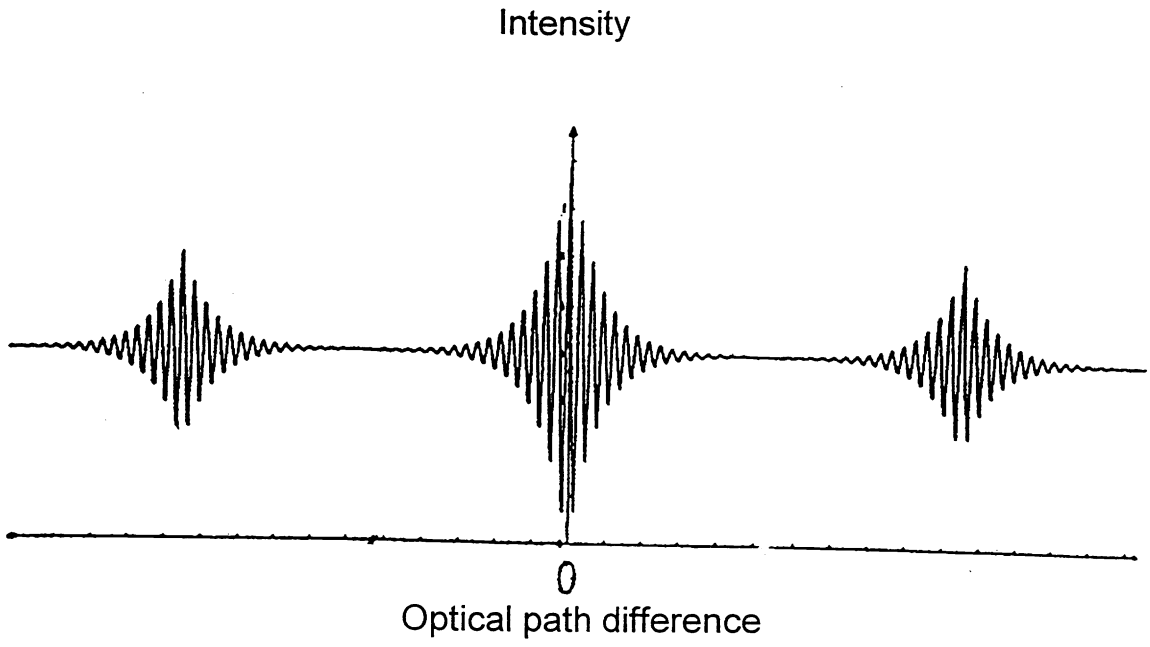

Fig. 4: Schematic interferogram obtained using a multimode laser diode operating above threshold.

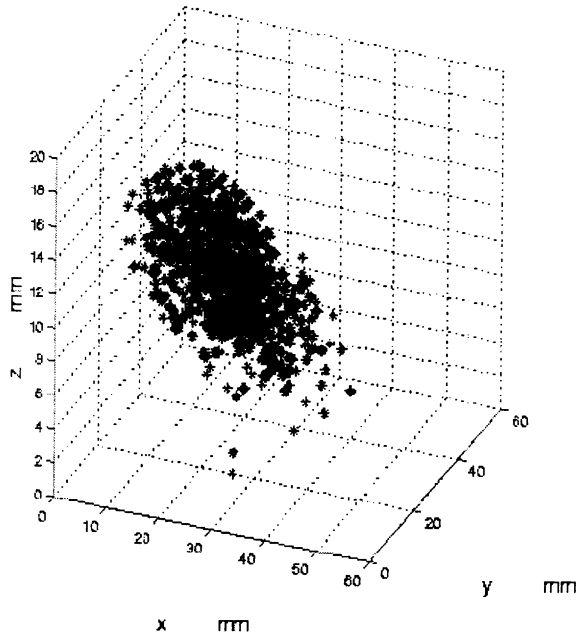

Fig. 5: 3D plot of the disc.

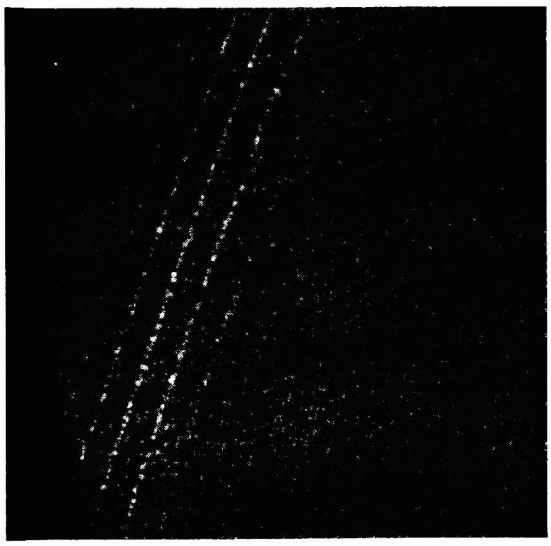

x=0mm

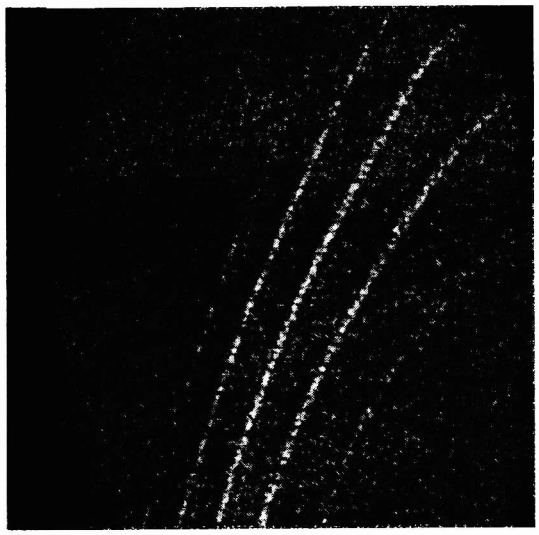

x=3mm

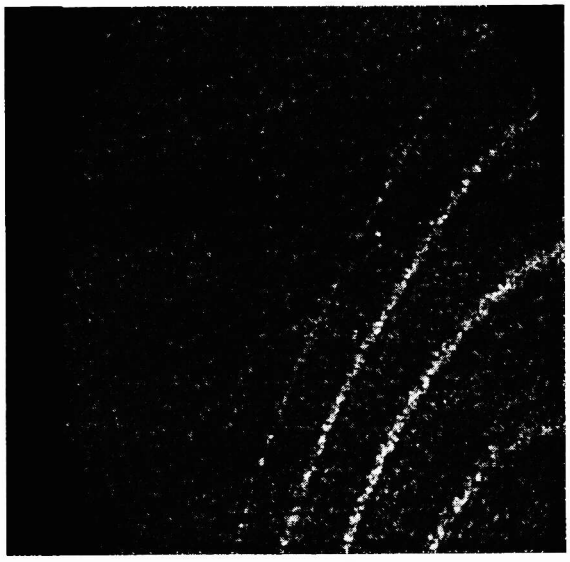

x=5.7mm

Fig. 6: Low coherence speckle fringes at different positions on the object surface. x represents the distance that the reference mirror has moved between images.

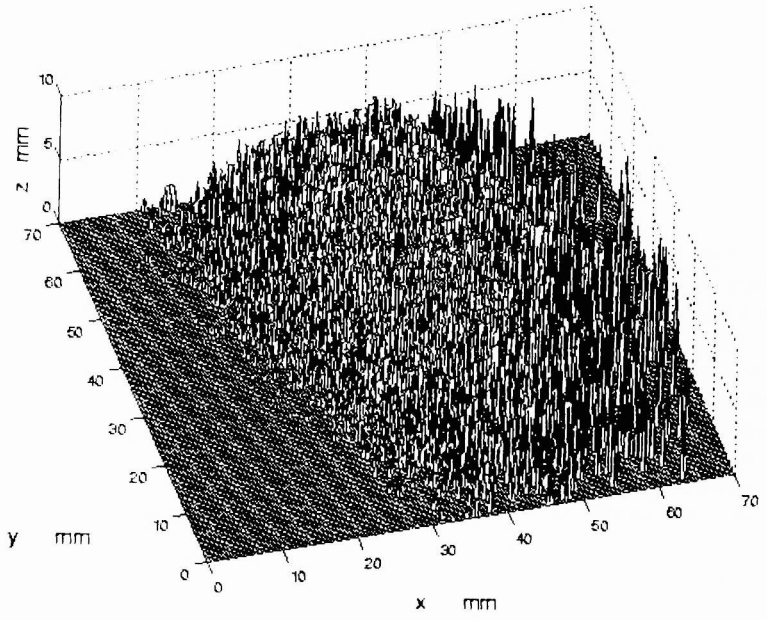

Fig. 7: 3D representation of the gas turbine blade.